Utilization of Altimetry Satellite Data in Investigating the Energy Potential of Tidal Current

Sony Junianto[a, *], Ika Purnamasari[b], Muhammad Nizar Habibi[c], Muhammad Zulfiqar Daffa[d], Nehemia Bagas Yudiprasetyo[d],

[a]Departemen Teknik Mekanika dan Energi, Politeknik Elektronika Negeri Surabaya
Kampus PENS, Jalan Raya ITS, Sukolilo, Surabaya 60111
[b]Departemen Agroteknologi, Fakultas Pertanian, Universitas Jember
Jalan Kalimantan No 37, Sumbersari, Jember 68121
[c]Departemen Teknik Elektro, Politeknik Elektronika Negeri Surabaya
Kampus PENS, Jalan Raya ITS, Sukolilo, Surabaya 60111
[d]Departemen Teknik Kelautan, Fakultas Teknologi Kelautan, Institut Teknologi Sepuluh Nopember
Kampus ITS, Jalan Raya ITS, Sukolilo, Surabaya 60111
*E-mail: sony@pens.ac.id

Abstract

Indonesia has a theoretical potential of tidal currents energy of 287 GW. The area that has the high potential is in the strait area. The tidal current has kinetic energy that can be converted into electricity using a Tidal Currents Energy Conversion System (TCECS). One of the potential straits is the Molo Strait. To determine the characteristics of tidal currents in the Molo Strait, local numerical modeling was carried out using tidal data and verified using publicly available field data. The equation used in local numerical modeling is the equation derived from the 3-dimensional Navier-Stokes equation by looking at the horizontal coordinates. The results of this modeling may be used to determine the power density and the type of turbine technology that is suitable to be applied in the Molo Strait. This paper reports that the Molo Strait has different two-way currents flow at high and low tides. In addition, the maximum mechanical power density at the potential point, coordinates (-8.625242°,119.805644°), in the spring and neap tides of the Molo Strait are 5.47 kW/m^2, 5.18 kW/m^2, 0.59 kW/m^2 and 0.7 kW/m^2, respectively. These may be calculated into mechanical power after determining the type and dimensions of the turbine technology.

Keywords: Tidal Current Energy, Energy Potential, Density Power, Current Flow

Abstrak

Indonesia secara teoritis mempunyai potensi energi arus laut sebesar 287 GW. Daerah yang mempunyai potensi tinggi berada di daerah selat. Arus laut memiliki energi kinetik yang dapat diubah menjadi listrik menggunakan pembangkit listrik tenaga arus laut (PLTAL). Salah satu selat yang potensial adalah Selat Molo. Untuk mengetahui karakteristik arus laut di Selat Molo, dilakukan pemodelan numerik lokal dengan menggunakan data pasang surut dan diverifikasi menggunakan data lapangan yang tersedia secara publik. Persamaan yang digunakan dalam pemodelan numerik lokal merupakan persamaan turunan dari persamaan Navier-Stokes 3 dimensi dengan melihat koordinat horizontal. Hasil pemodelan ini dapat digunakan untuk menentukan kepadatan daya dan jenis teknologi turbin yang cocok diterapkan di Selat Molo. Hasil penelitian ini melaporkan bahwa Selat Molo mempunyai aliran arus dua arah yang berbeda pada saat pasang dan surut. Selain itu, rapat daya mekanik maksimum pada titik potensial, koordinat (-8.625242°,119.805644°), pada pasang surut purnama dan perbani, Selat Molo adalah 5,47 kW/m^2, 5,18 kW/m^2, 0,59 kW/m^2 dan 0,7 kW/m^2. Ini dapat dihitung menjadi energi mekanik setelah menentukan jenis dan dimensi teknologi turbin.

Kata kunci: *Energi Arus Laut, Potensi Energi, Rapat Daya, Kecepatan Arus Laut*

1. Introduction

The theoretical potential of tidal currents energy in Indonesia reaches around 287 GW [1]. However, nowadays this potential has not been utilized to generate electricity. Therefore, the implementation of tidal currents energy in Indonesia needs to be done quickly with the aim of increasing the capacity of renewable power plants. For this reason, the stages before implementation need to be carried out both in the analysis of local potential to determining the type of technology [2].

The first step that needs to be done in the implementation process is the selection of potential locations [3]. Some of these locations have been found through a global study that was carried out by the Ministry of Energy and Mineral Resources together with Indonesian Ocean Energy Association in 2014 [4]. Based on that study, there are about ten potential straits in Indonesia. In addition, the existence of potential users or loads needs to be considered to select the potential location for implementing the tidal currents energy [5]. To analyze specifically and comprehensively that location, local analysis is proposed [6].

This analysis needs to be done because each potential strait has different characteristics of tidal currents therefore the technology needs to be adapted to these characteristics. In addition, the marine environment such as waves, water depth and the morphology of the seabed are also different for each potential strait [7]. Due to these factors, the Molo Strait is a potential location selected in this paper. This strait has a relatively high potential [4] and there are locations for residents who can utilize electricity from Tidal Currents Energy Conversion System (TCECS) in the vicinity.

This paper presents the results of a local analysis of the Molo Strait. This analysis is in a study of the potential for tidal currents, and mechanical power densitay. To determine the potential for mechanical power in the Molo Strait, TCECS is needed to convert the kinetic energy [8]. This local analysis in the Molo Strait may be used as a reference in conducting local analysis on other potential straits.

This analysis uses local numerical modeling with boundary layers set to describe the condition of the marine environment [9]. The results of this numerical modeling are in a time series which is used to calculate the mechanical power density. After knowing the character of the tidal currents in the Molo Strait, the appropriate type of turbine can be determined. Based on the results of research by Junianto et al [8], the conversion can use the horizontal axis turbine or the vertical axis turbine. The results of these analyzes are presented in several chapters that can provide information regarding the study of TCECS implementation in the Molo Strait.

2. Material and Method

2.1 Local Numerical Modeling

This numerical modeling was carried out locally and viewed in 2 dimensions picture, with the object of research being the Molo Strait. This strait has a relatively high energy potential for tidal currents in the global modeling that is explained before [4]. To find out the characteristics of the tidal currents in the strait, local numerical modeling has been done. This modeling was carried out using software that used tidal theory in analyzing tidal currents flow that described hydraulic principles or described physical flow phenomena [10].

The physical phenomenon of flow was obtained from numerical calculations of (1) – (4) which were non-linear equations to calculate the velocity of tidal currents. The equation was derived from the 3-dimensional Navier-Stokes equation by looking at the horizontal coordinates. For those, transformation was carried out into sigma coordinates (s) to provide a horizontal layer shape that will follow the pattern or shape of the waters that are the object of this simulation [11].

$$\frac{\partial u}{\partial x}+\frac{\partial v}{\partial y}+\frac{\partial w}{\partial z}=0 \tag{1}$$

$$\frac{\partial u}{\partial t}+\frac{\partial uu}{\partial x}+\frac{\partial uv}{\partial y}+\frac{\partial uw}{\partial z}=-\frac{1}{\rho}\frac{\partial p}{\partial y}+\frac{1}{\rho}\frac{\partial \tau xx}{\partial x}+\frac{1}{\rho}\frac{\partial \tau yx}{\partial y}+\frac{1}{\rho}\frac{\partial \tau zx}{\partial z}+g_x \tag{2}$$

$$\frac{\partial v}{\partial t}+\frac{\partial vu}{\partial x}+\frac{\partial vv}{\partial y}+\frac{\partial vw}{\partial z}=-\frac{1}{\rho}\frac{\partial p}{\partial y}+\frac{1}{\rho}\frac{\partial \tau xy}{\partial x}+\frac{1}{\rho}\frac{\partial \tau yy}{\partial y}+\frac{1}{\rho}\frac{\partial \tau zy}{\partial z}+g_y \tag{3}$$

$$\frac{\partial w}{\partial t}+\frac{\partial wu}{\partial x}+\frac{\partial wv}{\partial y}+\frac{\partial ww}{\partial z}=-\frac{1}{\rho}\frac{\partial p}{\partial z}+\frac{1}{\rho}\frac{\partial \tau xz}{\partial x}+\frac{1}{\rho}\frac{\partial \tau yz}{\partial y}+\frac{1}{\rho}\frac{\partial \tau zz}{\partial z}+g_z \tag{4}$$

where:

t	: time
x, y, z	: the coordinate axes of the longitudinal, transverse, and vertical directions
u, v, w	: instantaneous velocity of flow in the x, y, z direction
g_x, g_y, g_z	: acceleration due to gravity in x, y, z directions

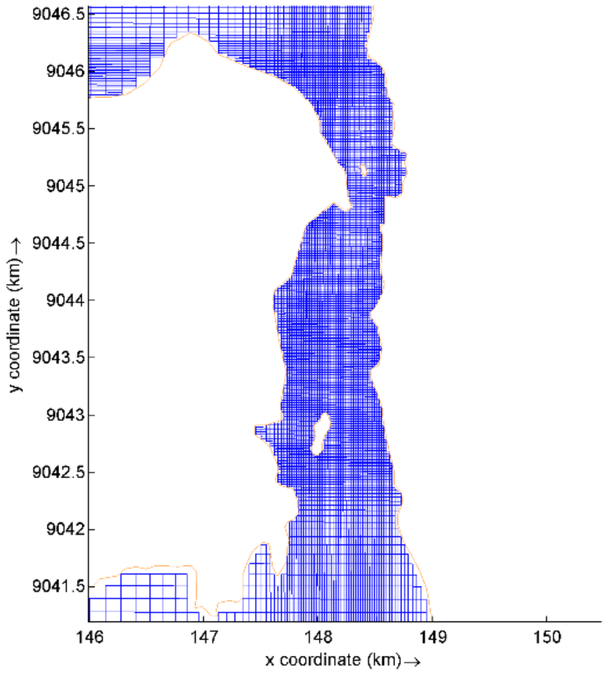

Fig. 1. Grid and Open Boundary of Molo Strait

In this numerical modeling, the application of the four equations was begun with using grid system for the Molo Strait. This simulation used a spherical coordinate system which was the position of the direction and height following the contour line of the earth's surface defined by latitude with vertical coordinates and longitude with horizontal coordinates. The results of meshing in the Molo Strait are shown in Fig. 1.

After that, the Molo Strait model was defined for each side by using boundary conditions which were a description of the external influence or the surrounding area on the model [12]. The Molo Strait used two types of boundary conditions, namely open boundaries and closed boundaries. The close boundaries were the islands surrounding area and meteorological data. While the border with the northern and southern parts of the open sea, the Molo Strait model was defined as an open boundaries.

2.2 Numerical Verification

This chapter describes the results of numerical modeling verification. This verification was carried out to ensure that the settings of numerical modeling of the Molo Strait produce tidal currents velocity data that are close to field conditions. Because there is no Molo Strait field measurement data in publication, the verification was carried out using the Alas Strait object which has field measurements data [13]. This type of verification is one way that may be done to justify numerical modeling settings when field or experimental data are unknown [7].

By using the equations in the previous chapter, the Alas Strait was modeled in software and simulated by numerical rules. The Alas Strait model used 3 open boundaries, i.e. in the north and south of the water using forcing type astronomic of main tidal constituents (M2, S2, K1, O1) obtained from the TPXO 8.0 Global Inverse Tide Model. This numerical setting was verified by field survey data [13].

The numerical results of the Alas Strait as a verifier in this modeling show that the modeled water level elevation with the measurement data has a mean sea level (MSL) difference of 0.07 m, as shown in Fig. 2. Phase changes can be modeled well, and water level elevation also has a relatively small difference in amplitude when compared to data from field measurements (surveys). These indicate having a strong, positive similarity relationship therefore the numerical settings of the Alas Strait can be used to the Molo Strait.

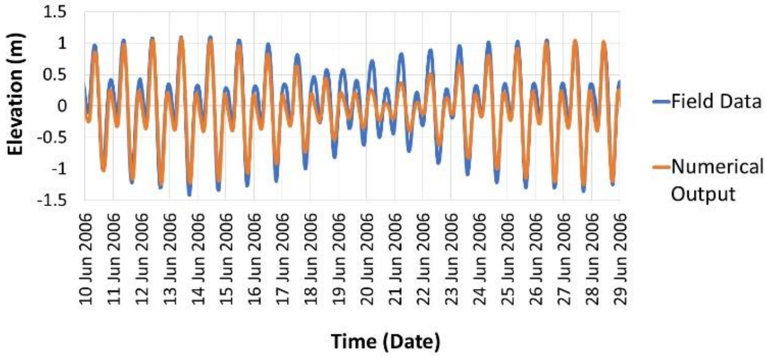

Fig. 2. Numerical Verification Using Field Data of the Alas Strait

3. RESULT AND DISCUSSION

The results of the numerical modeling of the Molo Strait are presented in this chapter. The results of this modeling are obtained after the settings in the software are verified which results are discussed in the previous chapter. The results are velocity of tidal currents in the Molo Strait with several observation points. The position of these points is reported in Table I. Each observation point was observed under spring tide and neap tide conditions. These two conditions are data samples with high and low tidal currents. These representative conditions can be seen in Fig. 3. The results of the Molo Strait modeling show the formzal number of 0.61 for the open boundary water level in the north and 0.5 in the south. From these results, this strait has a mixed tidal type, predominantly semi-diurnal.

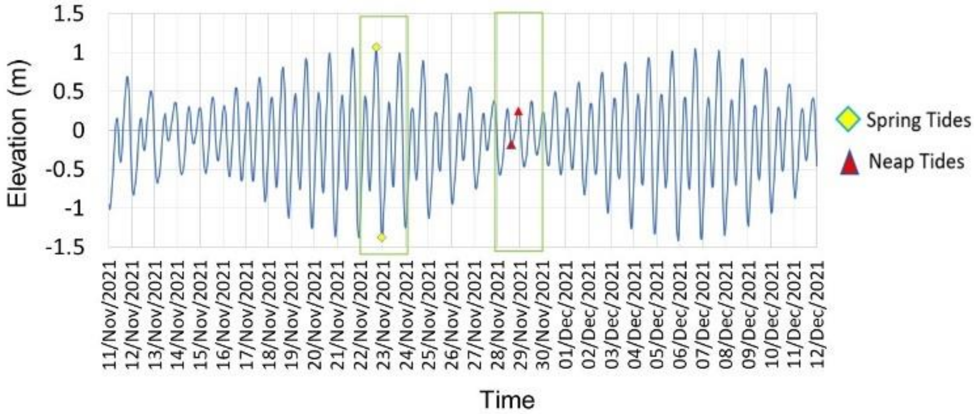

Fig. 3. Elevation of Tides in Molo Strait

Table 1. Observation Point Coordinate

Observation Point	Coordinate	
	Latitude	Longitude
1	-8,624255°	119,806018°
2	-8,624262°	119,806272°
3	-8,625655°	119,806092°
4	-8.625571°	119,806373°
5	-8,624680°	119,804714°
6	-8.625236°	119,805217°
7	-8.625242°	119,805644°
8	-8,625929°	119,806920°
9	-8.626115°	119,807402°
10	-8.626292°	119.807821°

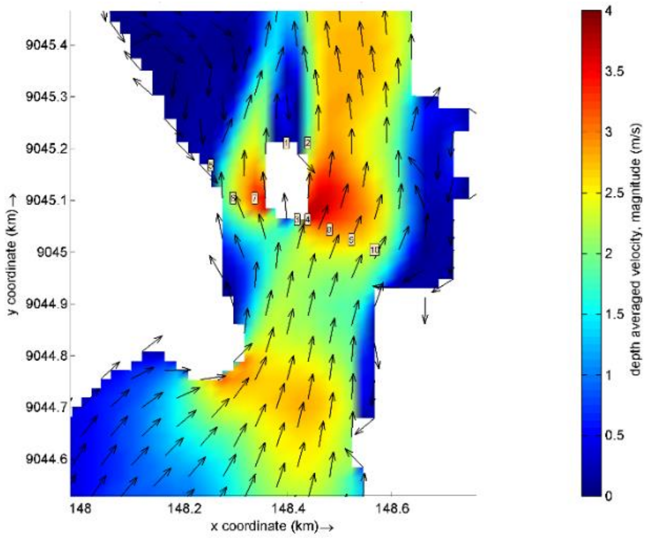

Fig. 4. The Velocity and Direction of Tidal Current in The Molo Strait During the High Spring Tides

Fig. 4 shows the results of numerical modeling in spring tide condition. Currentsly, the direction of the tidal currents moves from south to north. In addition, the figure shows the color gradation of the distribution of tidal currents at each observation point. The red color indicates the velocity of the tidal currents at that point is higher than the velocity of the tidal currents at the blue one. The velocity at each observation point can be seen in Fig. 5. The figure shows that Observation Point 4 has the highest tidal currents velocity compared to other observation points. This point allows to produce more electricity than other observation points.

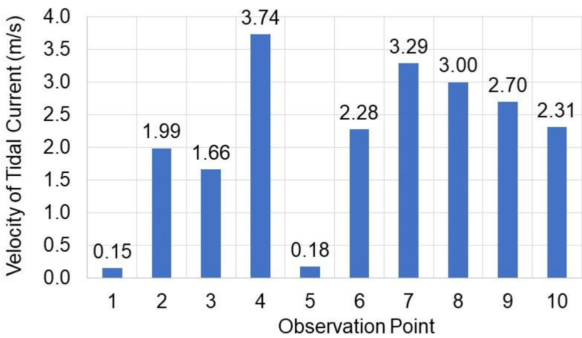

Fig. 5. Velocity of Tidal Current Distribution in Molo Strait During The High Spring Tides

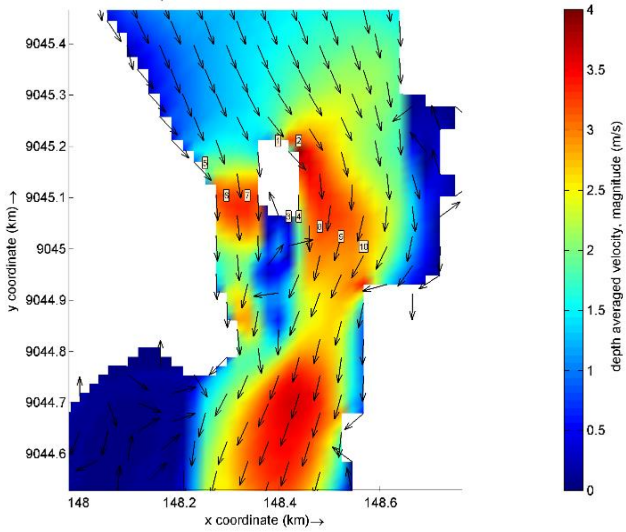

Fig. 6. The Velocity and Direction of Tidal Current in The Molo Strait During The Low Spring Tides

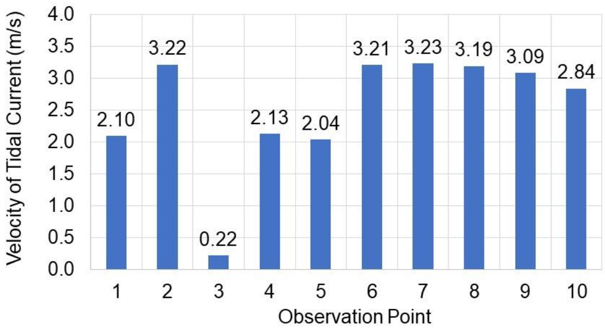

Fig. 7. Tidal Current Velocity Distribution in Molo Strait During The Low Spring Tides

At low spring tide, the patterns of tidal currents and their velocity show different results from the high spring tide. These results are shown in Fig. 6. In this figure, the tidal currents move from north to south, which shows the opposite direction of currents at high tide. In the figure of the distribution of tidal currents, there are areas that have eddies around Observation Point 3. Therefore, the velocity of tidal currents at that point is low, marked in blue. Then, Fig. 7 shows the distribution of tidal currents at each observation point. Based on these data, the highest velocity of tidal currents is at Observation Point 2.

Furthermore, the numerical modeling was carried out in negligible tidal conditions. In this condition, the neap tides in are much lower than during the spring tides. The direction of tidal currents at neap tides resembles the direction of currents during spring tides. When the high neap tides, the tidal currents move from south to north (Fig. 8). Meanwhile, at low tide, the tidal currents move from north to south (Fig. 10). In this condition, the tidal currents have a lower velocity than during the spring tides. The distributions of tidal currents at neap tides are shown in Fig. 9 and Fig. 11.

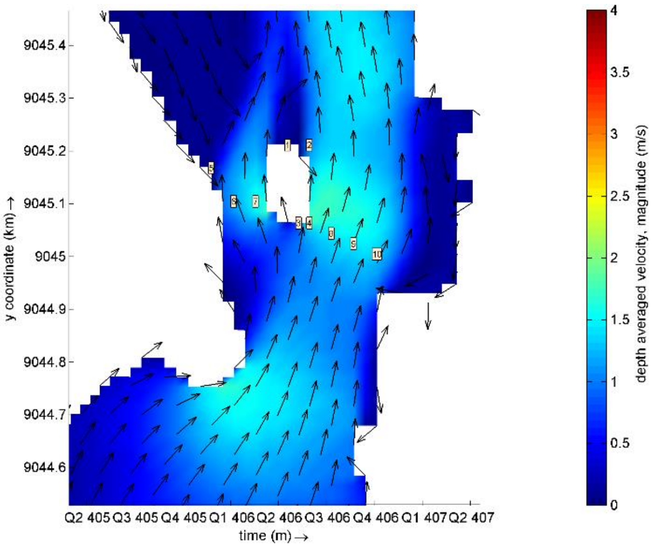

Fig. 8. The Velocity and Direction of Tidal Currents in The Molo Strait During The High Neap Tides

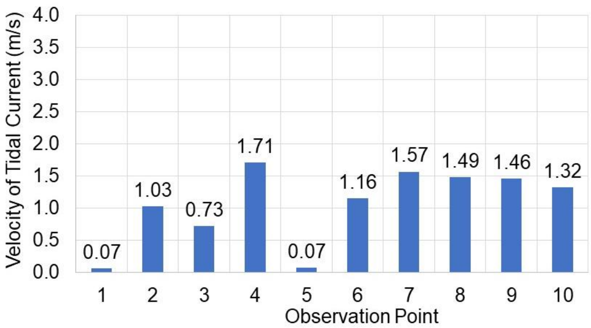

Fig. 9. Tidal Currents Velocity Distribution in Molo Strait During The High Neap Tides

Data on the velocity of tidal currents at each observation point at spring and neap tides conditions are processed to determine the percentage of total sample. The distribution is processed according to velocities above 1 m/s and 0.7 m/s. Each of these distributions has a percentage as shown in the graphs in Figs.12 and 13. From the two graphs, the largest percentage is at Observation Point 7, which is 86% for velocity above 1 m/s and 90% for velocity above 0.7 m/s. In other words, this point has the highest probability of turbine operation when the turbine has a cut-in speed of 1 m/s or 0.7 m/s.

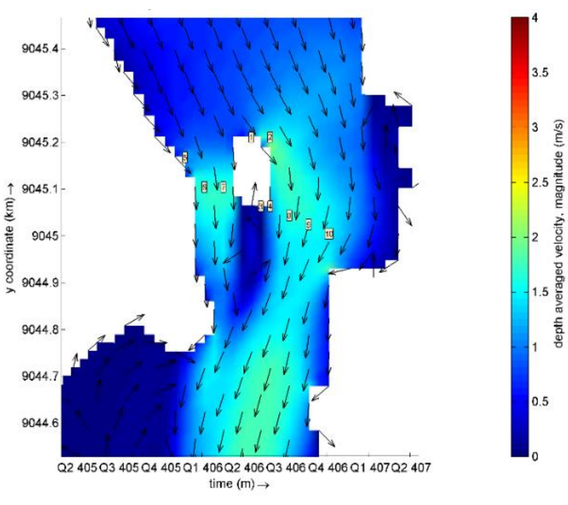

Fig. 10. The Velocity and Direction of Tidal Current in The Molo Strait During The Low Neap Tides

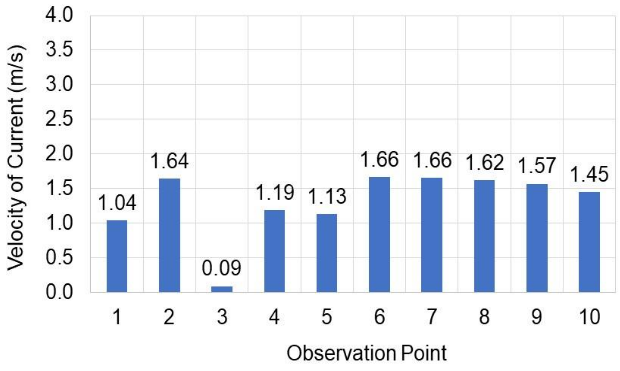

Fig. 11. Tidal Currents Velocity Distribution in Molo Strait During The Low Neap Tides

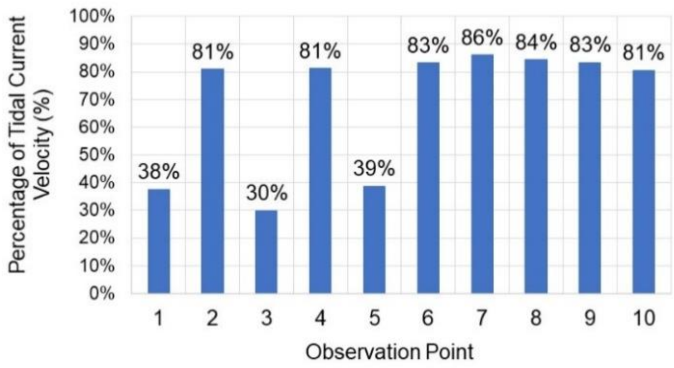

Fig. 12. Percentage of Tidal Current Velocity Above 1 m/s in Molo Strait

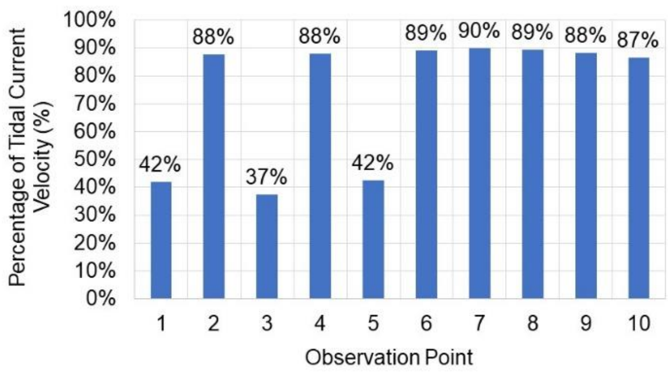

Fig. 13. Percentage of Tidal Current Velocity Above 0.7 m/s in Molo Strait

According to the maximum speed value at Observation Point 7, the maximum power density value, P/A, can be determined by calculation (5) at that point. Assuming an efficiency, C_p, of 30%, the maximum mechanical power density, P_t/A, can be determined for each condition. At high spring tides, the maximum mechanical power density is 5.47 kW/m^2 and the maximum mechanical power density at low spring tides is 5.18 kW/m^2. Meanwhile, at high neap tides, the maximum mechanical power density at Observation Point 7 is 0.59 kW/m^2 and 0.7 kW/m^2 at low neap tides.

$$\frac{P_t}{A} = \frac{1}{2} C_p \rho v^3 \tag{5}$$

The characteristics of tidal currents in the Molo Strait have been shown through previous figures. The direction of tidal currents in the strait is alternating, from south to north during high tide conditions and from north to south during low tide conditions. For this flow, the vertical axis tidal currents turbine is more suitable because the turbine can extract energy from any direction of fluid flow, in contrast to the horizontal axis currents turbine which only extracts energy from the fluid flow coming from the front of the turbine cross section [7]. From the results of this numerical modeling, the type of turbine, both its axis type and its cut in speed may be determined.

4. Conclusion

The Molo Strait is one of the straits in Indonesia that has the potential for tidal currents energy. Local numerical modeling was carried out to determine local characteristics in the strait. The setting in the modeling has been well verified using field data on the Alas Strait. The results of this modeling show that the relatively high potential in the Molo Strait is located at Observation Point 7, which is at coordinates (-8.625242°,119.805644°). The percentage of occurrence at this potential point is 86% for tidal currents above 1 m/s and 90% for tidal currents above 0.7 m/s. This condition indicates that a suitable turbine technology is a turbine with a low cut-in speed. In addition, the tidal currents in the Molo Strait have a two-way direction of flow, i.e from south to north at high tide and from north to south at low tide where this condition provides a suitable performance for vertical axis tidal currents turbine. This Observation Point 7 also shows the potential mechanical power density during spring and neap tides at 5.47 kW/m^2, 5.18 kW/m^2, 0.59 kW/m^2 and 0.7 kW/m^2, respectively.

5. Acknowledgement

The authors would like to convey a great appreciation to the Ministry of Education, Culture, Research and Technology, Republic of Indonesia, for granting the research fund.

6. References

[1] Mukhtasor, “Ocean energy in Indonesia”, Ocean Energy Workshop, Jakarta, Indonesia, November 2012

[2] S. Rahmawati, H. Mutsuda, Y. Doi, “Numerical estimation for tidal-current energy resources in Indonesia”, Autumn Conference of The Japanese Society of Naval Architects and Ocean Engineers, Tokyo, Japan, 2015

[3] S. Rahmawati, Study on characteristics of tidal current energy and ocean environmental pollution at Indonesia archipelago, Dissertation, 2017

[4] Mukhtasor, Susilohadi, Erwandi, W. Pandoe, W, “Indonesia's ocean energy potential”, Research and Development Agency of the Ministry of Energy and Mineral Resources and the Indonesian Ocean Energy Association, 2014

[5] M.A.J.R. Quirapas, A. Taeihagh, Ocean renewable energy development in Southeast Asia: opportunities, risks and unintended consequences, Renewable and Sustainable Energy Reviews, 2021, Vol. 137, pp. 110403

[6] N. P. Purba, J. Kelvin, R. Sandro. S. Gibran, R. A. I. Permata, F. Maulida, M. K. Martasuganda, Suitable locations of ocean renewable energy (ORE) in Indonesia Region – GIS approached, Energy Procedia, 2015, Vol, 65, pp. 230-238

[7] S. Junianto, Mukhtasor, R. W. Prastianto, C. H. Jo, Effects of demi-hull separation ratios on motion response of tidal current turbines-loaded catamaran, Ocean Systems Engineering, 2020, Vol. 10 (1), pp. 87-110

[8] S. Junianto, Mukhtasor, R. W. Prastianto, W. Wardhana, Motion response analysis for tidal current energy platform: quad-spar and catamaran types. China Ocean Engineering, 2020, Vol. 34, pp. 677-687

[9] J. Thiebot, D. S. Coles, A. C. Bennis, N. Guillou, S. Neill, S. Guillou, M. Piggott, Numerical modelling of hydrodynamics and tidal energy extraction in the Alderney Race: a review, Philosophical Transactions A, 2020, Vol. 378 (2178), pp. 20190498

[10] J. G. Rueda-Bayona, A. F. Osorio, A. Guzman, Set-up and input dataset files of the Delft3d model for hydrodynamic modelling considering wind, waves, tides, and currents through multidomain grids, Data in Brief, 2020, Vol. 28, pp. 104921

[11] V. Ramos, R. Carballo, J. V. Ringwood, Application of the actuator disc theory of Delft3D-FLOW to model far-field hydrodynamic impacts of tidal turbines, Renewable Energy, 2019, Vol. 139, pp. 1320-1335

[12] M. B. R. Topper, Guidance for numerical modelling in wave and tidal energy, The University of Edinburgh, March 2010

[13] Mukhtasor, L. B. Sugito, Sujantoko, Prelimenary modeling for assesing tidal stream energy potential at the Alas Strait, Indonesia, International Journal of Offshore and Coastal Engineering, 2017, Vol. 1(2), pp. 86-93